

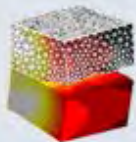
Distributed Damage and Enhanced Permeability in Confined Brittle Materials under Triaxial Compression

Michael Ortiz

Caltech, Pasadena CA

In collaboration with: Maria Laura De Bellis, Gabriele Della Vecchia,
Anna Pandolfi, DICA, Politecnico di Milano

ECCOMAS Thematic Conference



*IV International Conference on Computational Modeling
of Fracture and Failure of Materials and Structures*

CFRAC 2015

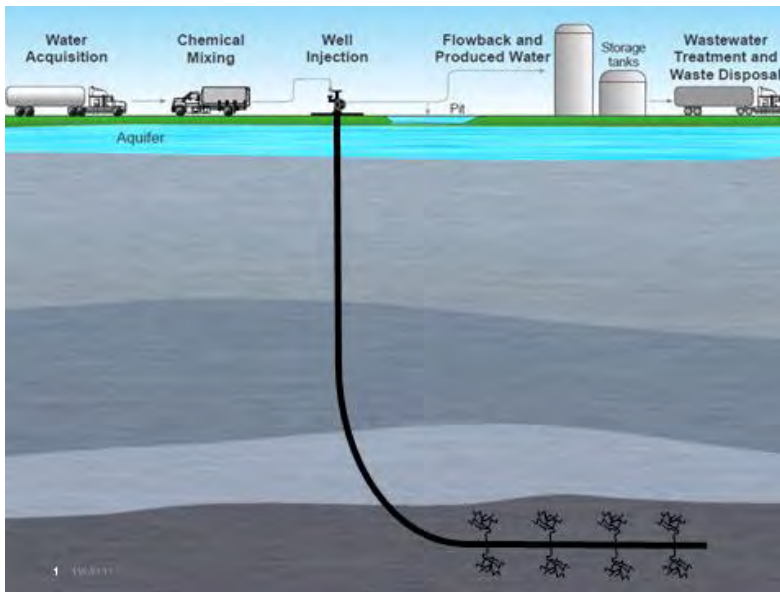
3 - 5 June 2015 (Cachan), France



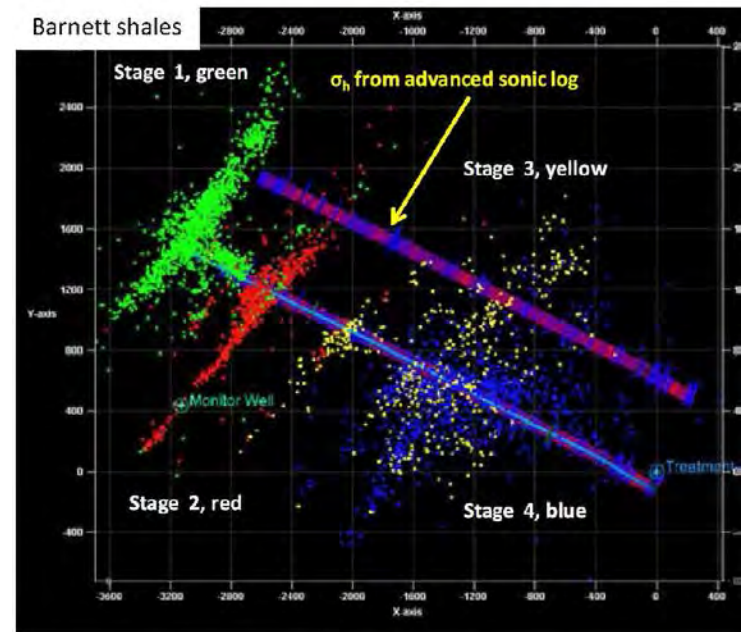
IACM Special Interest Conference

Motivation: Hydraulic Fracture (HF)

Hydraulic fracture: Example of extreme complexity, uncertainty, coupling to the environment...



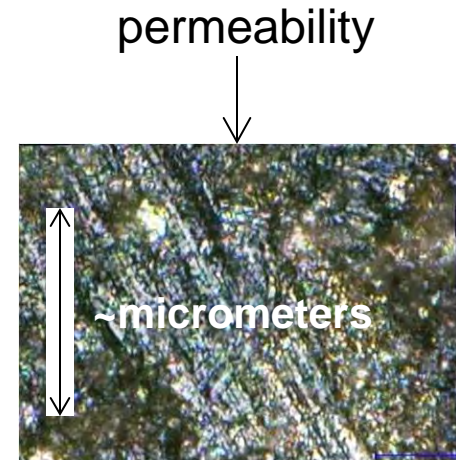
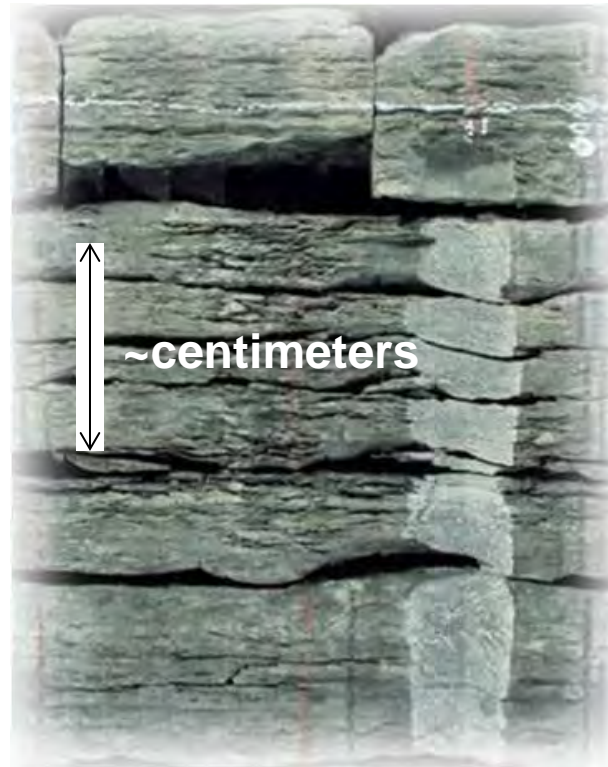
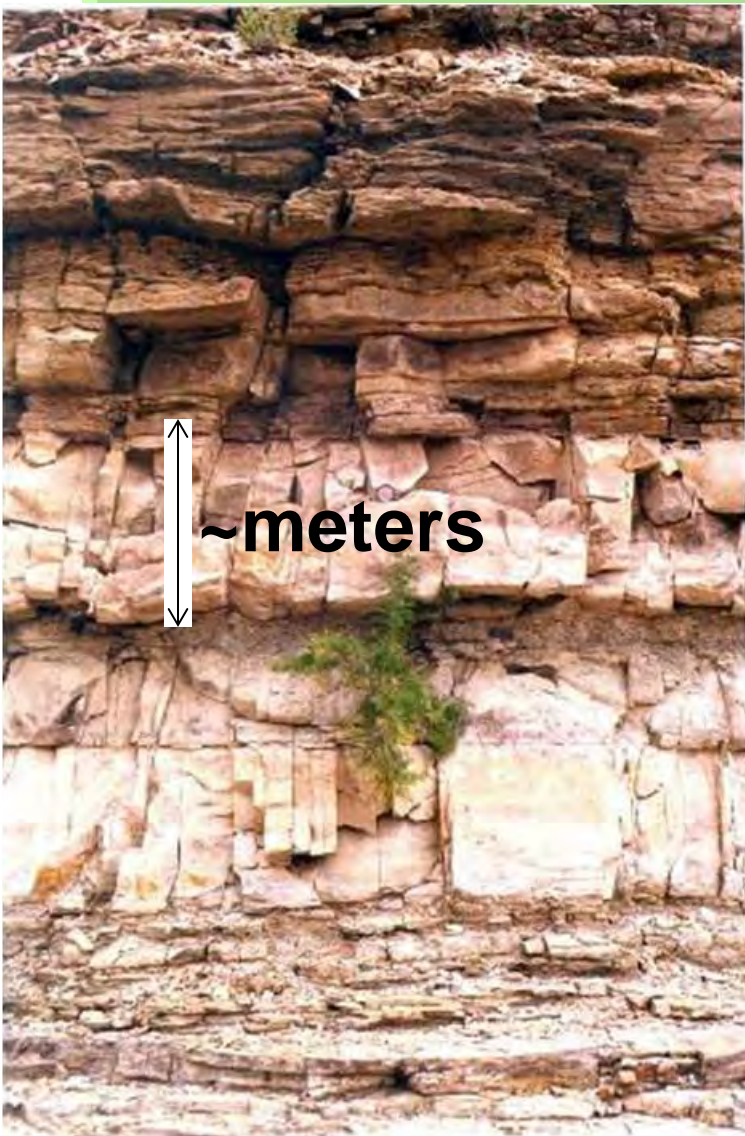
Schematic of hydraulic fracture by horizontal drilling (S. Green and R. Suarez-Rivera, AAPG Geoscience Technology Workshop, 2013)



Complex pattern of hydraulic fractures generated during fracking mapped from acoustic emissions (R. Wu *et al.*, SPE-152052-MS, 2012)

HF as a multiscale phenomenon

Subgrid length scales!



← complex
multiscale
rock
formations

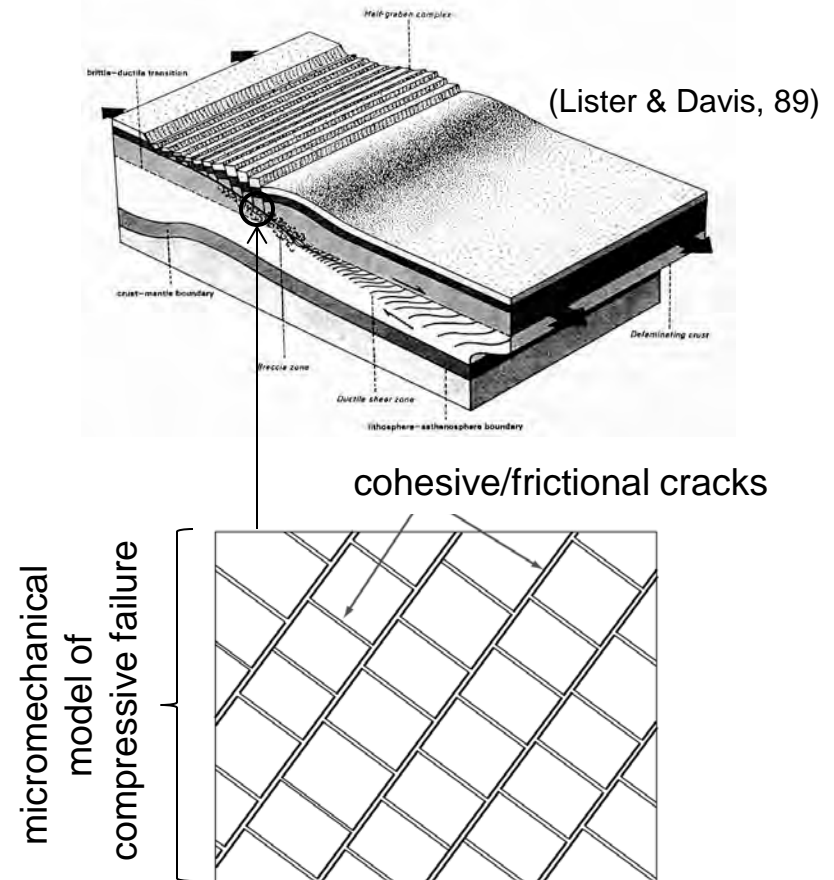
S. Green, R. Suarez-Rivera
Schlumberger Innovation Center
AAPG Geoscience Technology Workshop
July 16, 2013

Modeling and simulation challenges, objectives

- **Hydraulic fracture** is characterized by:
 - **Distributed fracture** under **triaxial compression**
 - **Complexity** of fracture patterns, geology
 - **Multiscale** phenomena: From 10^2 m to 10^{-6} m (subgrid)
 - **Multiphysics**: coupling to permeability, flow
 - **Uncertainty quantification**: limited data
- **Past models** of HF:
 - Mathematically sharp cracks in homogeneous elastic media
 - Newtonian/non-Newtonian flow through parallel planes
- **Past models** of compressive fracture:
 - ‘Abstract’ empirical/phenomenological distributed damage models
 - No explicit connection with microstructure geometric/evolution
 - Coupling to elasticity and permeability through empirical laws...
- **Objective: Multiscale model** of compressive damage/permeability based on **explicit constructions** of distributed fracture (recursive faulting)

Multiscale modeling of compressive damage

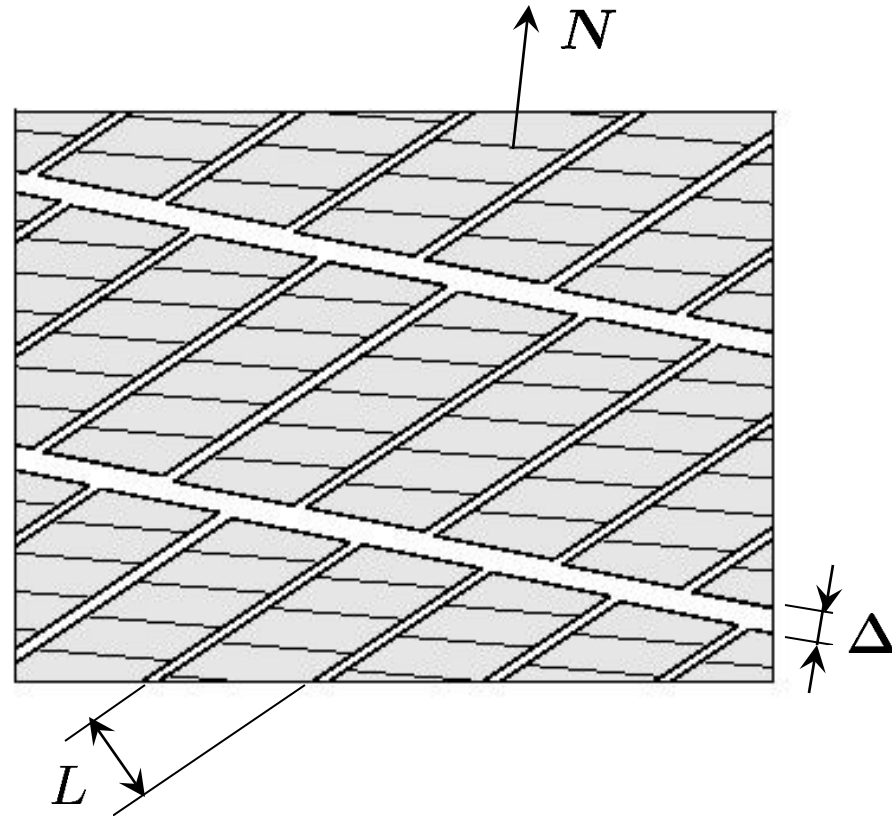
- Rocks in compression fail through complex 3D fracture patterns
- At the microscale: Multiple families of nested shear/frictional cracks
- Length scales from microscopic to geological
- Behavior of fracture system depends on behavior at both micro and macroscales:
 - Overall geometry of HF governed by macroscopic damage mechanics
 - **Permeability governed by fine detail of microstructure**
- **‘Abstract’ damage mechanics not enough: Multiscale modeling!**



Pandolfi, A., Conti, S. and Ortiz, M.,
J. Mech. Phys. Solids, **54**: 1972-2003, 2006

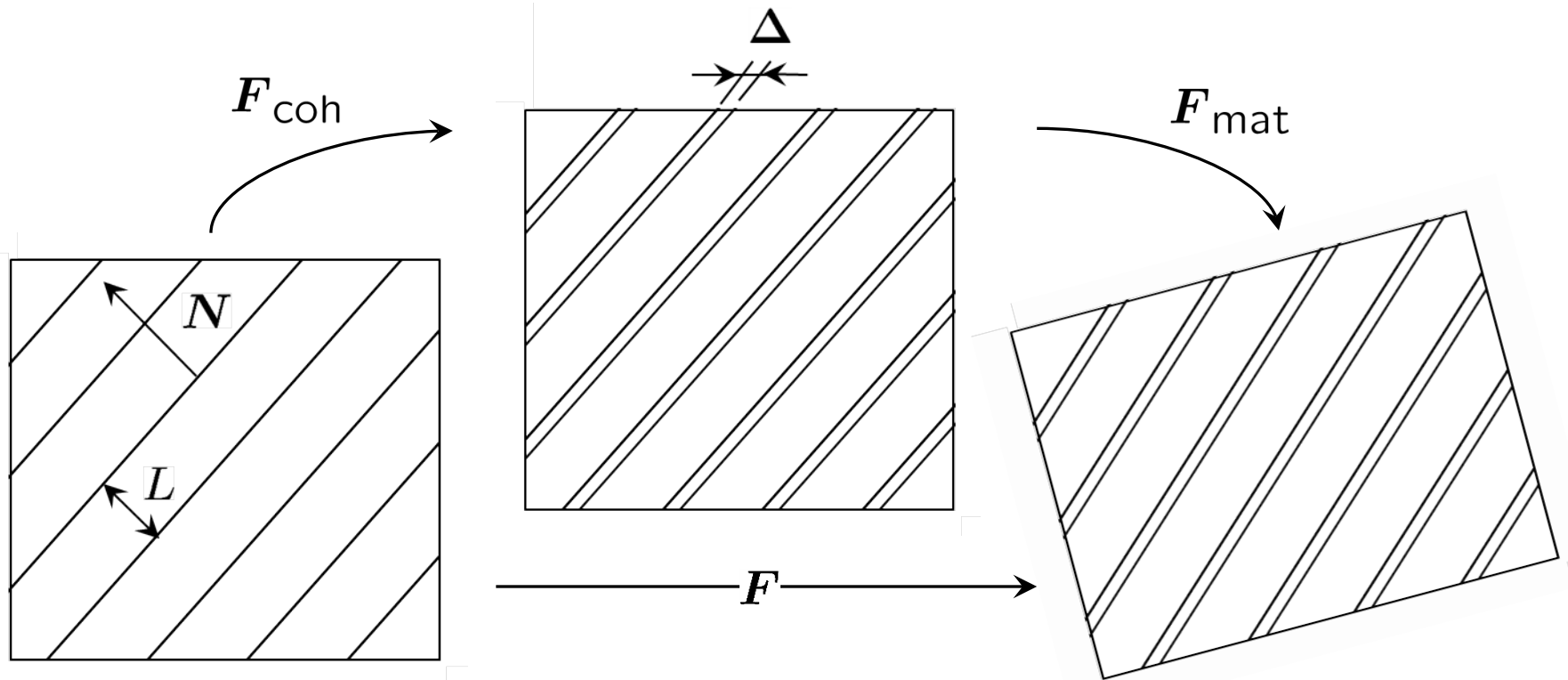
Multiscale model of compressive damage

- Special class of microstructures, consisting of **nested families of equi-spaced cohesive faults**. The matrix material can be elastic or inelastic (e.g., plastic)
- Each family of cohesive faults is characterized by an **orientation N** and a **spacing L** (both determined by the theory)
- The behavior of the faults (opening displacement Δ) is governed by a cohesive law (open fault) and Coulomb friction (closed fault).
- The faults may be pre-existing (geological) or nucleate during deformation.



Schematic of recursive-faulting construction (two families)

Single-fault model - Kinematics



- Deformation due to faults: $F_{\text{coh}} = I + \frac{1}{L} \Delta \otimes N$
- Total deformation: $F = F_{\text{mat}} F_{\text{coh}}$

Irreversible cohesive behavior

- Effective opening displacement [Ortiz & Pandolfi, 1999]:

$$\Delta = \sqrt{\Delta_N^2 + \beta^2 \Delta_S^2}$$

$$\Delta_N = \Delta \cdot \mathbf{N} > 0, \quad \Delta_S = |\Delta - \Delta_N \mathbf{N}|$$

- Cohesive energy

$$\Phi = \Phi(\Delta, q), \quad T = \frac{\partial \Phi(\Delta, q)}{\partial \Delta}$$

- Irreversibility: unloading to origin, use the maximum attained opening displacement q as internal variable with kinetic relations

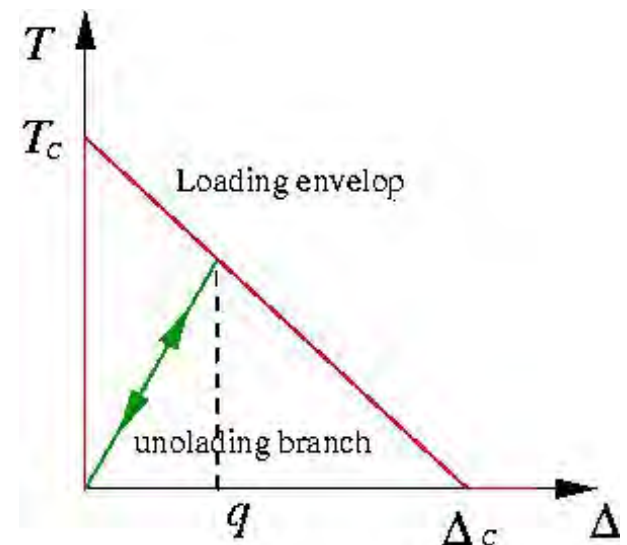
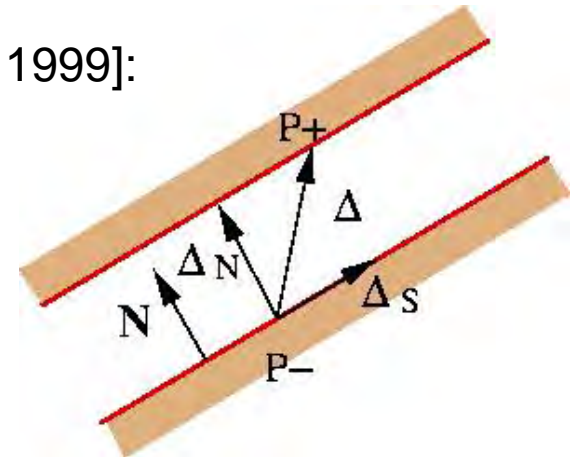
$$\dot{q} = \begin{cases} \dot{\Delta}, & \text{if } \Delta = q \text{ and } \dot{\Delta} \geq 0 \\ 0, & \text{otherwise} \end{cases}$$

- Variational update [Ortiz & Stainier, 1999]:

$$W_n(\mathbf{F}) = \inf_{\Delta, q} \left\{ W_{\text{mat}}(\mathbf{F}_{\text{mat}}) + \frac{1}{L} \Phi(\Delta, q) \right\}$$

subject to:

$$\Delta \cdot \mathbf{N} \geq 0, \quad q \geq q_n$$



Frictional contact and sliding

- Friction is concurrently present at faults with cohesion. Once faults loose cohesion, friction remains the only dissipation mechanism.
- Dual dissipation potential Ψ^* per unit surface [Pandolfi *et al.*, IJNME, 2002]

$$\Psi^*(\dot{\Delta}; \mathbf{F}, q, \Delta) = \mu \max \{0, -\mathbf{N} \cdot \mathbf{S} \mathbf{N}\} |\dot{\Delta}|,$$

- where \mathbf{S} is the 2nd PK stress tensor and $\mu = \tan \phi$ the friction coefficient
- Variational update [Ortiz & Stainier 1999, Pandolfi *et al.* 2006]:

$$W_n(\mathbf{F}) = \inf_{\Delta, q} \left\{ W^{\text{mat}}(\mathbf{F}_{\text{mat}}) + \frac{1}{L} \Phi(\Delta, q) + \frac{\Delta t}{L} \Psi^* \left(\frac{\Delta - \Delta_n}{\Delta t}; \mathbf{F}, q, \Delta \right) \right\}$$

subject to: $\Delta \cdot \mathbf{N} \geq 0, \quad q \geq q_n$

- PK stresses and tangent moduli follow as

$$\mathbf{P} = \frac{\partial W_n(\mathbf{F})}{\partial \mathbf{F}}, \quad D\mathbf{P} = \frac{\partial^2 W_n(\mathbf{F})}{\partial \mathbf{F} \partial \mathbf{F}}$$

Fault inception and optimal orientation

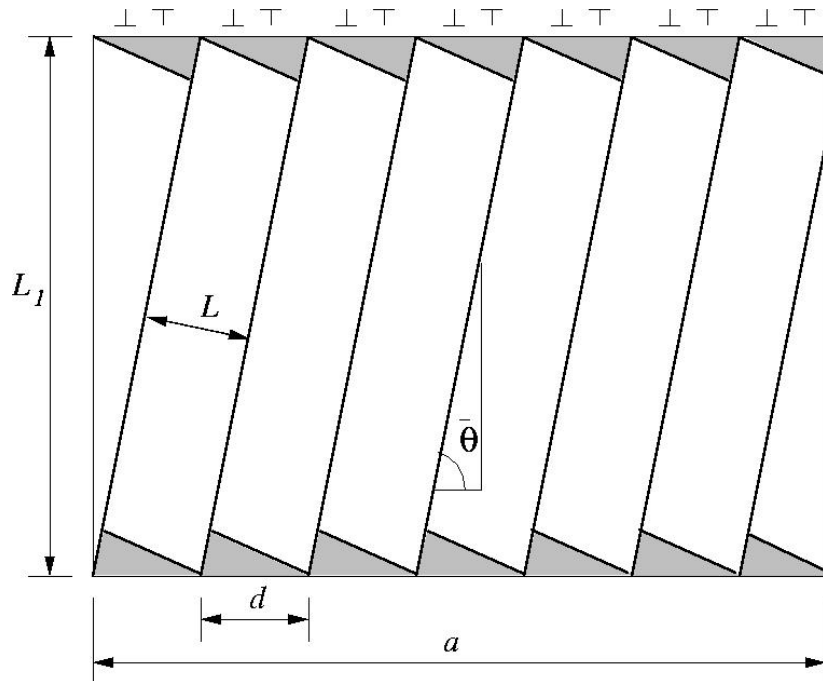
- Is the insertion of faults energetically favorable?
 - Test two end states of the material, without and with faults.
 - Chose the one resulting in the lowest incremental energy W_n .
- There is an energetically optimal orientation \mathbf{N} ? The optimal orientation is given by the solution of the extended constrained minimum problem

$$W_n(\mathbf{F}) = \inf_{\Delta, q, \mathbf{N}} \left\{ W_{\text{mat}}(\mathbf{F}_{\text{mat}}) + \frac{1}{L} \Phi(\Delta, q) + \frac{\Delta t}{L} \Psi^* \left(\frac{\Delta - \Delta_n}{\Delta t}; \mathbf{F}, q, \Delta \right) \right\}$$

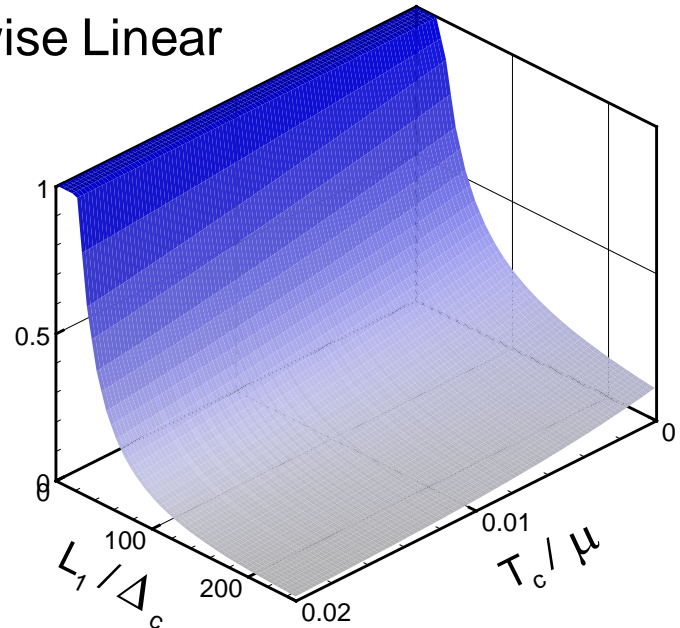
$$\text{subject to: } \Delta \cdot \mathbf{N} \geq 0 \quad q \geq q_n \quad |\mathbf{N}|^2 = 1$$

- The optimum \mathbf{N} is given by:
 - If faults open (tensile state): direction of maximum tensile stress
 - If faults slide (compressive state): normal to the plane of maximum shear, inclined of $\theta = \pi/4 - \phi/2$ with respect to the maximum principal stress direction (Mohr-Coulomb failure criterion)

Misfit energy and optimal fault separation



Piecewise Linear

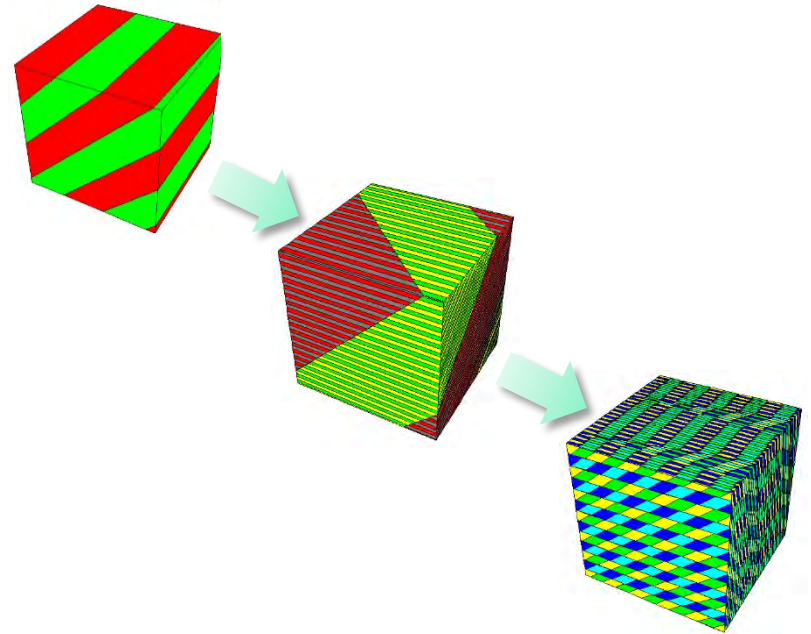


- Misfit energy: $E^{\text{mis}}(L_{n+1}) = \frac{C|\Delta|^2}{L_1} \frac{1}{L_{n+1}} \log \frac{L_{n+1}}{L_0}$
- Total energy:
$$W_n(\mathbf{F}) = \inf_{\Delta, q, L} \left\{ W^{\text{m}}(\mathbf{F}^{\text{m}}) + \frac{1}{L} \Phi(\Delta, q) + \frac{\Delta t}{L} \Psi^* \left(\frac{\Delta - \Delta_n}{\Delta t}; \mathbf{F}, q, \Delta \right) + E^{\text{mis}}(L) \right\}$$
- Optimize:
$$L_{n+1} = \Delta_c \exp \left[1 - \frac{L_1}{\Delta_c} \frac{T_c}{2\mu} \right]$$

Recursive faulting construction

- Once the first fault family has developed, the matrix between faults may experience a tensile/shear state resulting in further faulting on a sublevel.
- The matrix deformation gradient \mathbf{F}_{mat} at the first level can be in turn decomposed into further matrix and cohesive components governed by the single-family model
- Nested faulting of any depth can be implemented simply by calling the single-family model recursively (supported in C and C++ languages)

$$\mathbf{F} = \mathbf{F}_{\text{mat}}^{(1)} \mathbf{F}_{\text{coh}}^{(1)} \quad \text{Rank-1}$$
$$\mathbf{F}_{\text{mat}}^{(1)} = \mathbf{F}_{\text{mat}}^{(2)} \mathbf{F}_{\text{coh}}^{(2)} \quad \text{Rank-2}$$
$$\mathbf{F}_{\text{mat}}^{(2)} = \mathbf{F}_{\text{mat}}^{(3)} \mathbf{F}_{\text{coh}}^{(3)} \quad \text{Rank-3}$$



Optimality of sequential faulting

- Is sequential optimal faulting optimal? Are there other microstructures (fracture patterns) that are more efficient at relaxing the energy of a brittle solid under geostatic (triaxial) stresses?
- Recall: Quasiconvex envelop $W_{qc}(\mathbf{F})$ = smallest energy density/volume obtained by considering all possible microstructures (fracture patterns) consistent with macroscopic deformation \mathbf{F}
- $W_{qc}(\mathbf{F})$ describes the optimal (softest) effective macroscopic behavior of a brittle solid undergoing fracture under triaxial compression

Theorem [PCO'06] Assume no friction, and

$$W_{\text{mat}}(\mathbf{F}) = W_{\text{dev}}(\mathbf{F}_{\text{dev}}) + W_{\text{vol}}(J).$$

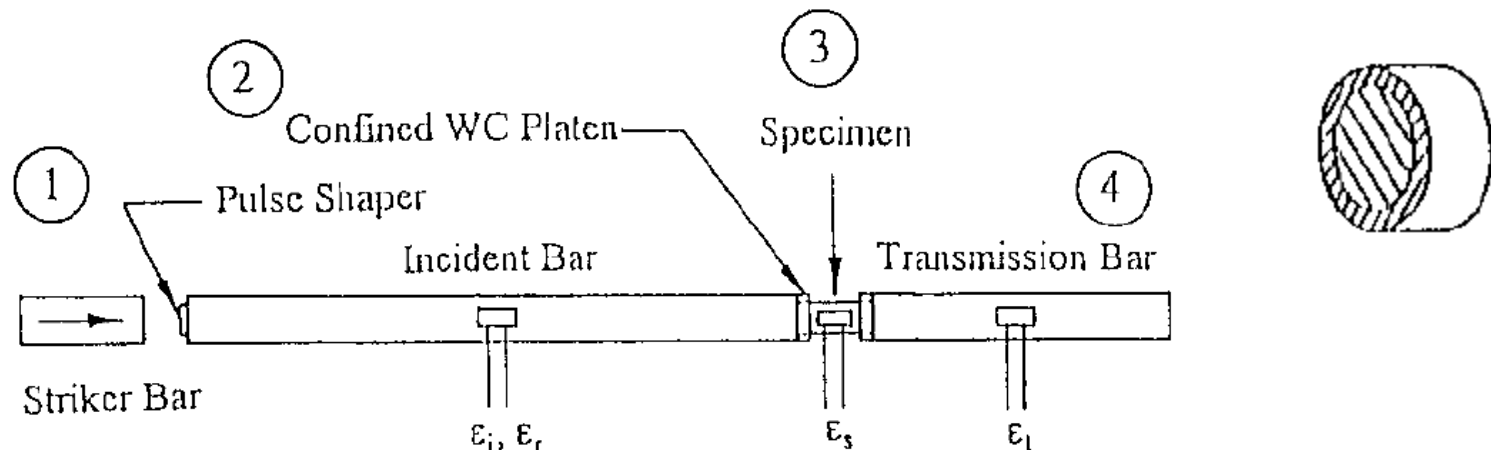
Then:
$$W_{qc}(\mathbf{F}) = \begin{cases} W_{\text{vol}}(J), & \text{if } J \leq 1, \\ 0, & \text{if } J > 1, \end{cases}$$

attained by sequential-faulting construction.

- Sequential faulting fully relaxes all geostatic deviatoric stresses!

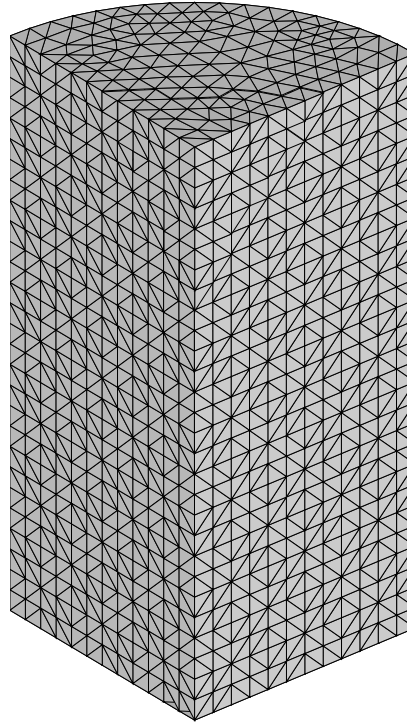
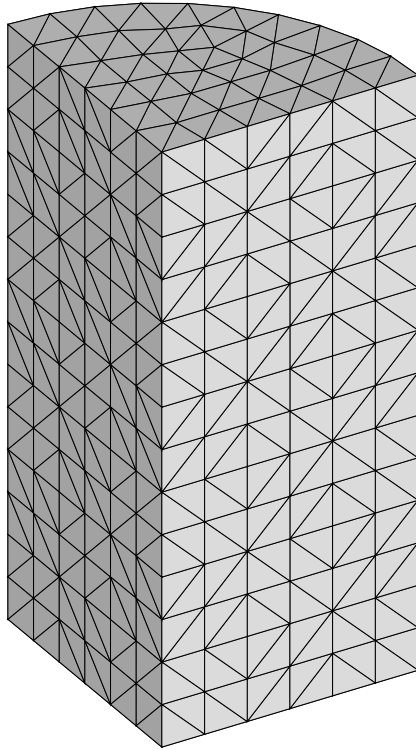
Experimental validation

- Refer to the experiments by Chen and Ravichandran on Sintered Aluminum Nitride (AlN) [Chen and Ravichandran, JAS, 1996].
- Special experimental technique to impose lateral confinement on AlN cylinder, by using a shrink-fit metal sleeve.
- Confinement increases the resistance and the ductility of the specimen, both in static and in dynamic case.



(Courtesy of G. Ravichandran)

Experimental validation



$$E = 310 \text{ GPa}$$

$$\nu = 0.237$$

$$T_c = 180 \text{ MPa}$$

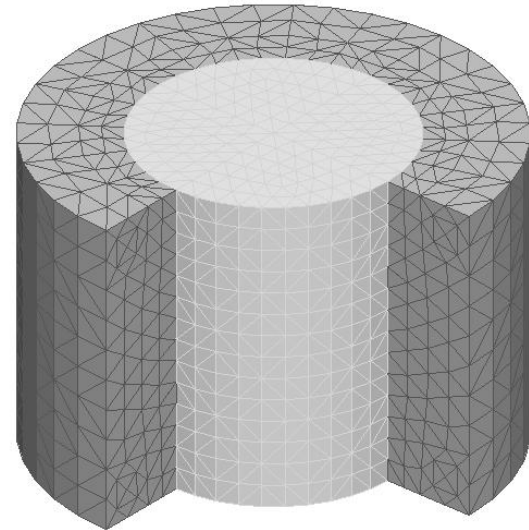
$$G_c = 162 \text{ N/m}$$

$$\beta^2 = 12$$

$$L_0 / L_c = 100$$

$$\rho = 3200 \text{ kg/m}^3$$

- Tetrahedral FE meshes of AlN specimen and steel sleeve
- Two mesh sizes to verify mesh-size insensitivity of calculations



Experimental validation

Experiments
(Chen and
Ravichandran '96)

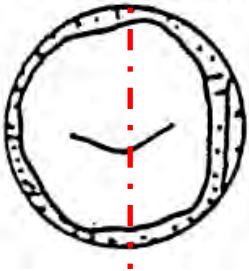
Top
view



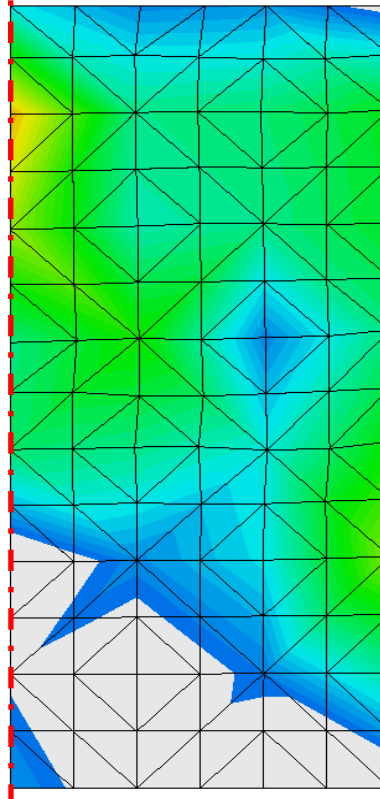
Cross
Section



Bottom
view



Damage
contour levels
Cross section

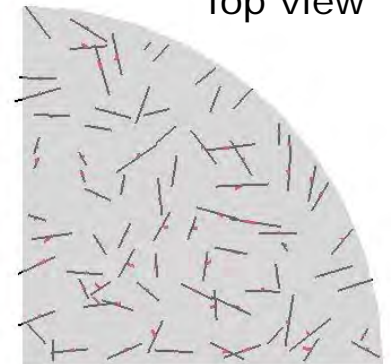


Planes of fracture (black) and opening (red)

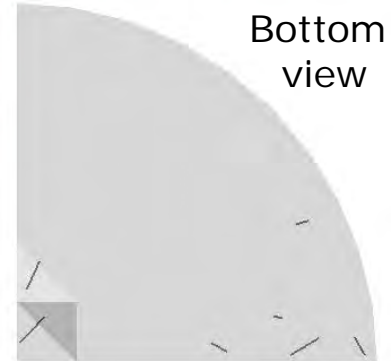
Cross section



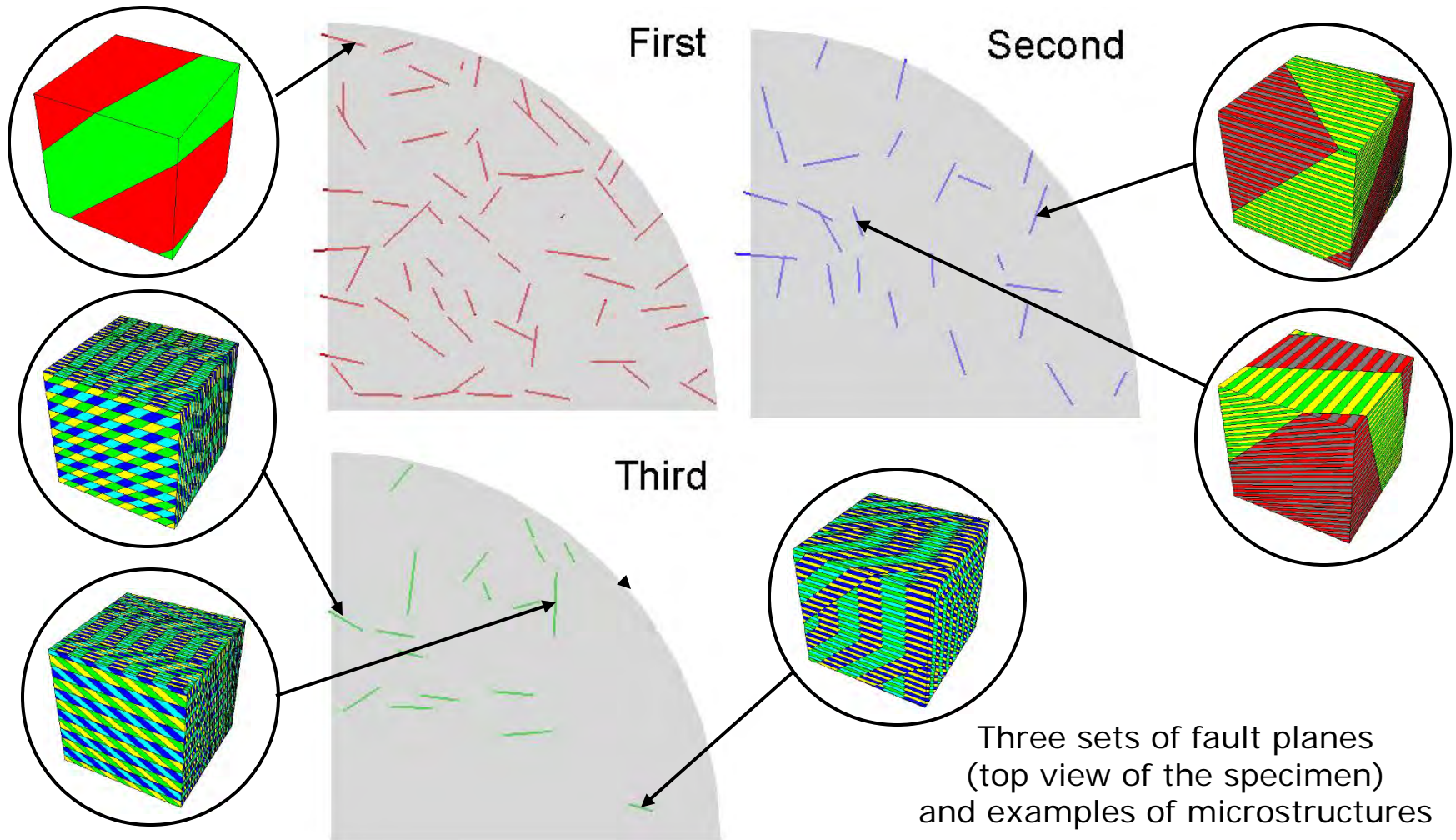
Top view



Bottom
view

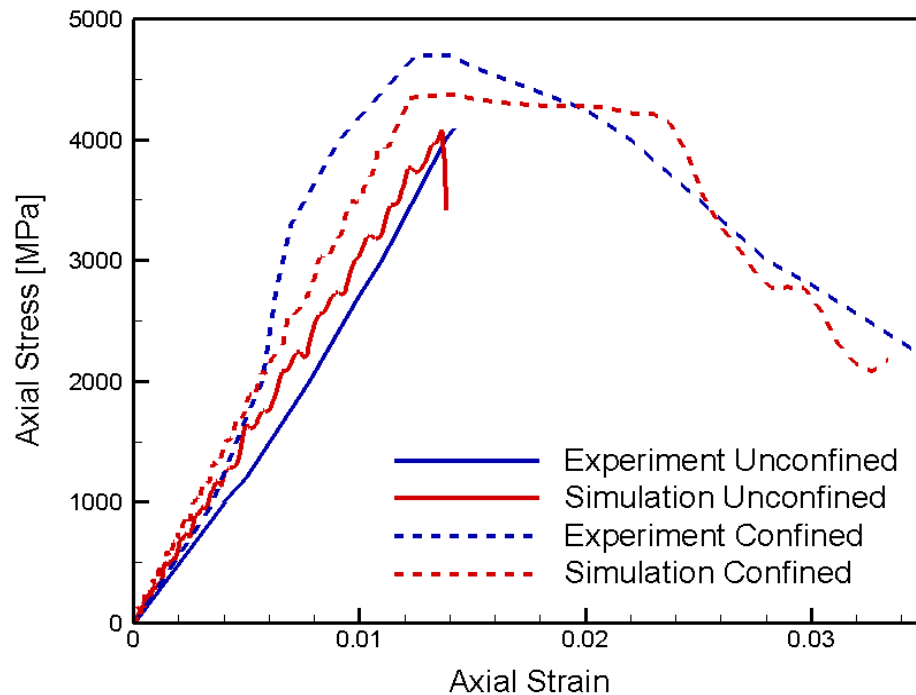


Experimental validation

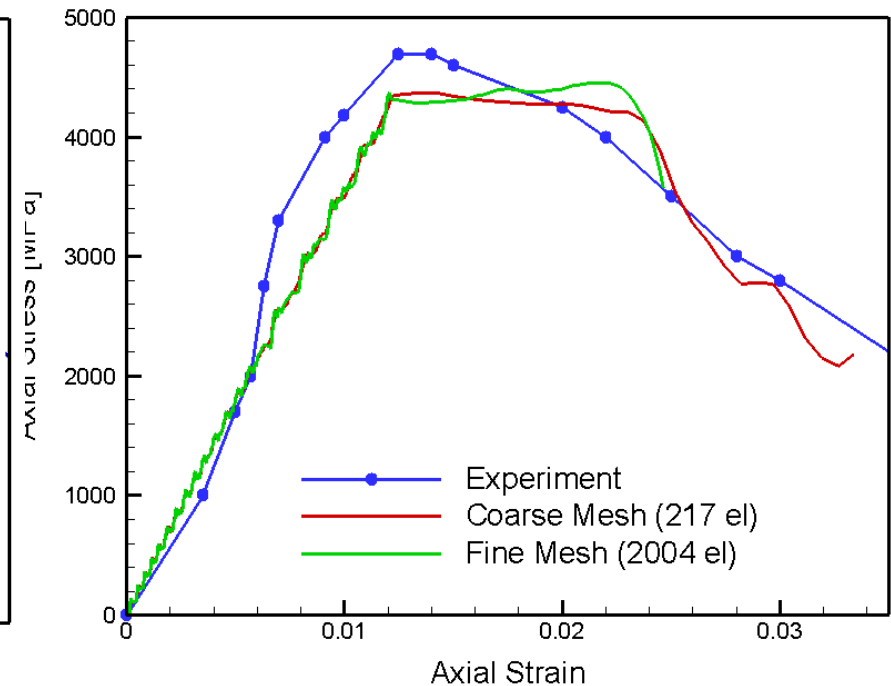


Experimental validation

Comparison with experiment
[Chen and Ravichandran, 1996]



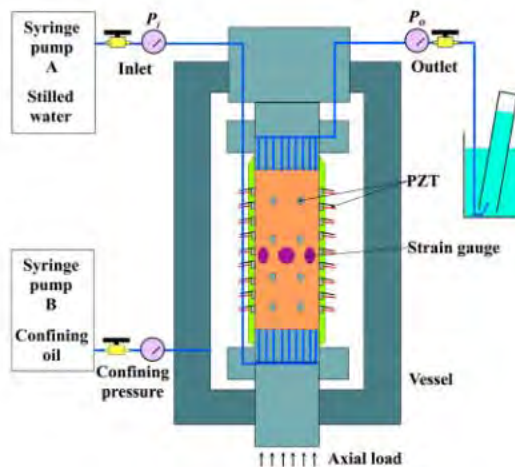
Mesh-size sensitivity



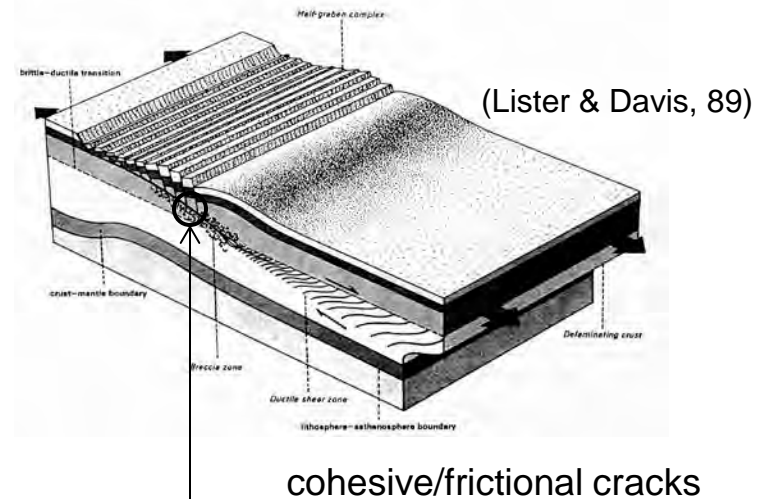
- Model captures brittle-to-ductile transition with increasing confinement
- Model results are mesh-size insensitive

Damage-enhanced permeability

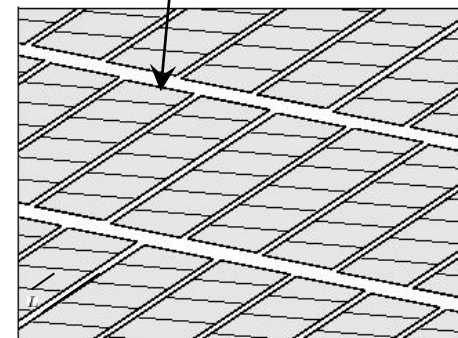
- Explicit **recursive-faulting** construction characterizes both **average macroscopic behavior** and **fine structure** of the fracture pattern at the microscale
- Can couple the predicted microscopic fracture geometry and evolution to **permeability model**



Lei et al., *Geophys. Res. Lett.*,
38, L24310, 2011



micromechanical
 model of
 compressive failure



Pandolfi, A., Conti, S. and Ortiz, M.,
J. Mech. Phys. Solids, **54**: 1972-2003, 2006

Porous media equations in finite kinematics

- Terzaghi's effective stress principle, p pore pressure: $\mathbf{P} = \mathbf{P}' + p\mathbf{J}\mathbf{F}^{-T}$
- Total porosity and permeability: $n = n_m + n_f$ $\kappa = \kappa_m + \kappa_f$
- Matrix porosity and permeability (Kozeni-Carman model)

$$n_m = 1 + \frac{1}{J}(n_0 - 1), \quad \kappa_m = C_{KC} \frac{(n_m)^3}{(1 - n_m)^2}$$

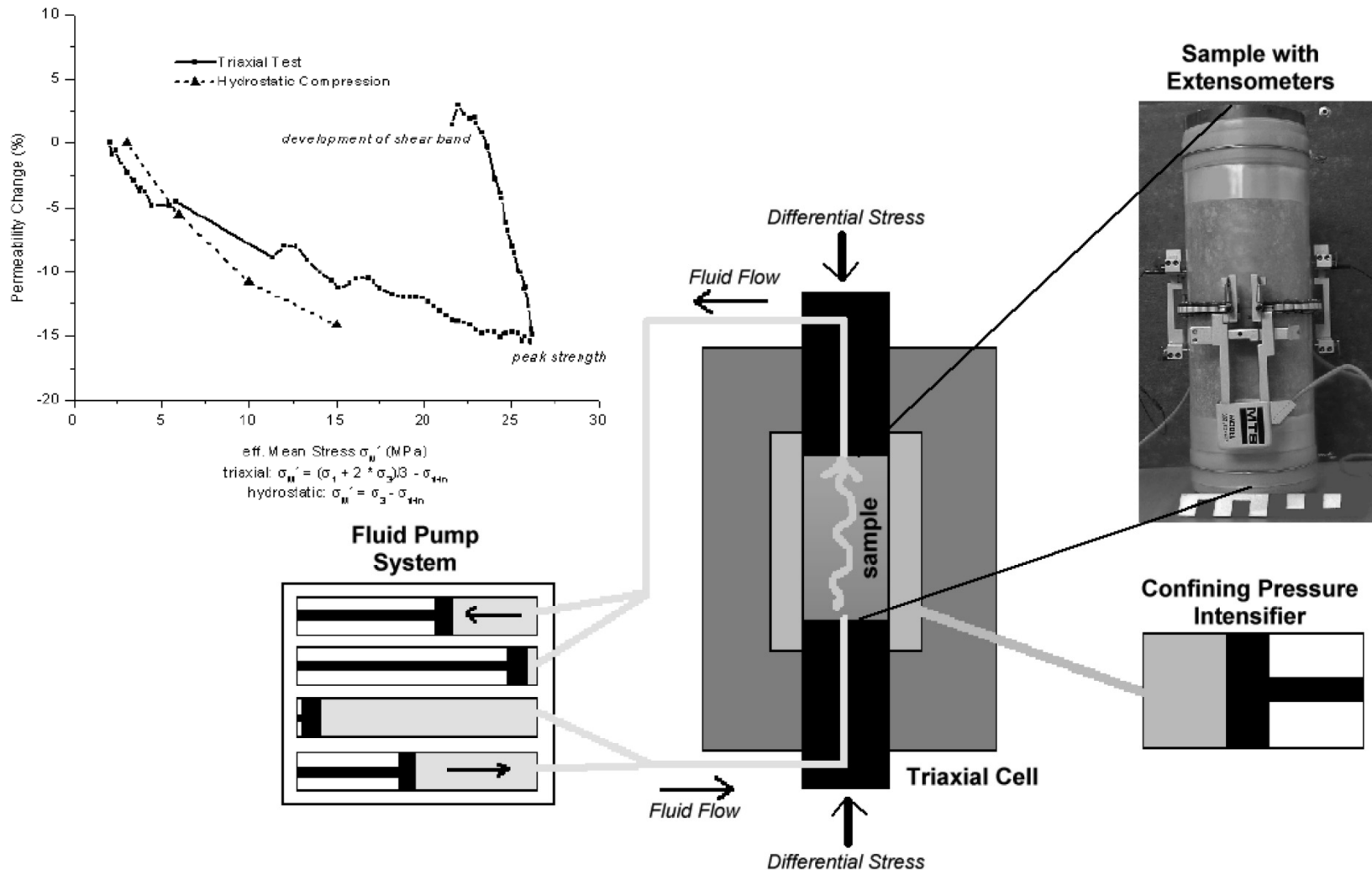
- Permeability due to fracture (laminar flow between parallel planes):

$$\kappa^f = \sum_{k=1}^Q \frac{\Delta_N^k}{L^k + \Delta_N^k} \frac{\Delta_N^{k^2}}{12} \left(\mathbf{I} - \underset{\substack{\uparrow \\ \text{fault-orientation dependence} \\ \text{(anisotropic permeability...)}}}{\mathbf{N}^k \otimes \mathbf{N}^k} \right)$$

\uparrow
 fault-opening dependence
 (effect of stress, pore pressure, friction...)

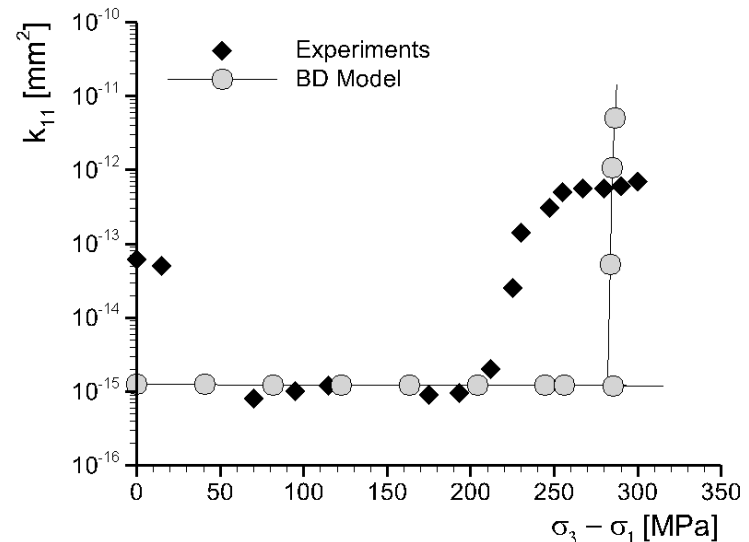
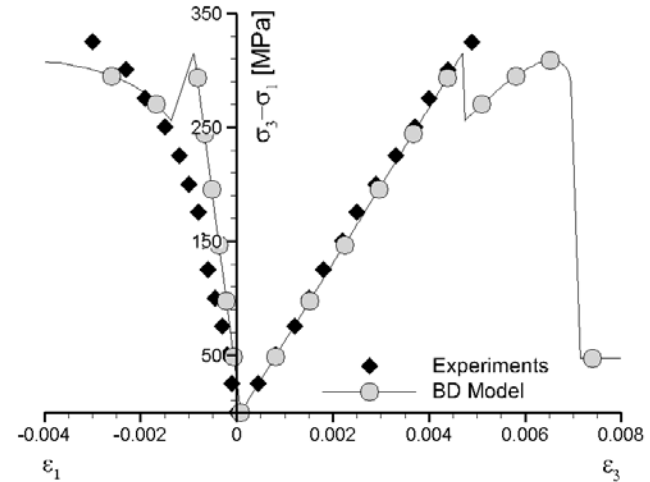
\uparrow
 fault-density dependence
 (specific fracture energy, size effect...)

Typical post-peak permeability behavior in rocks



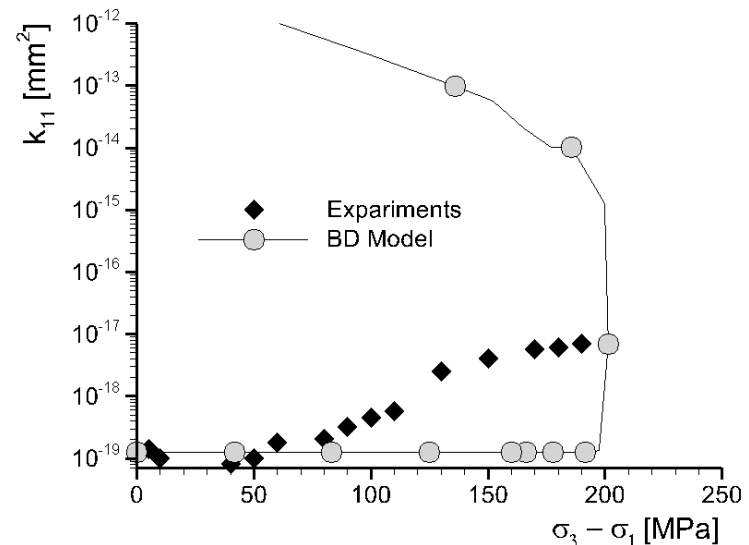
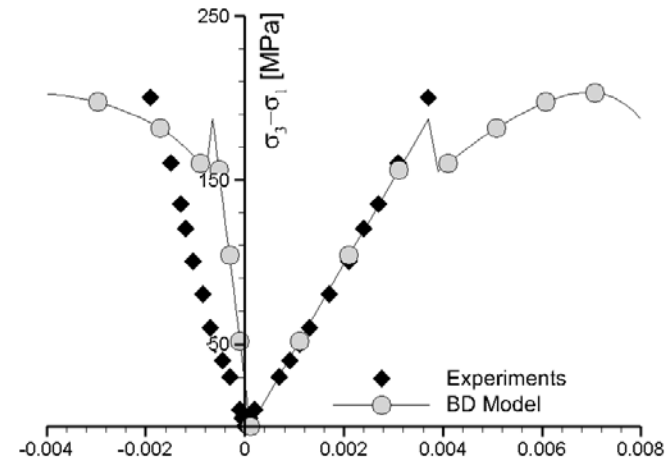
Material-point validation: Lac du Bonnet granite

- Experimental data from [Souley et al., 2001]
- Confinement 10 MPa
- Triaxial test up to the peak, with measurements of the permeability
- Missing material data on strength and fracture energy
- Satisfactory deviatoric stress versus axial and lateral strain
- Prediction of permeability shows sharp upturn after peak, corresponding to usual experimental trend



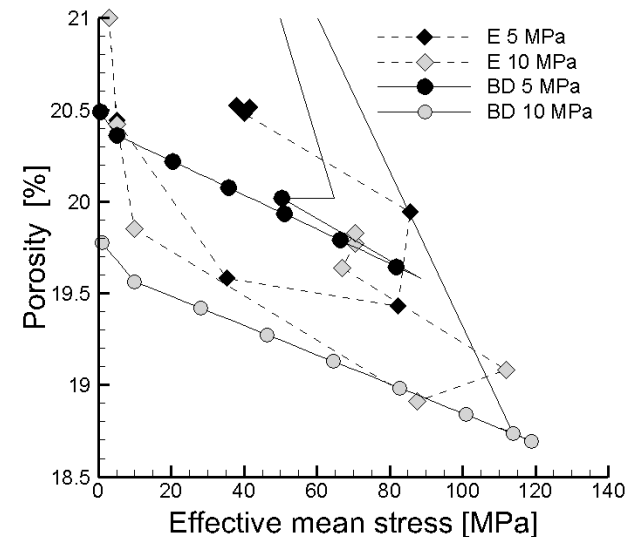
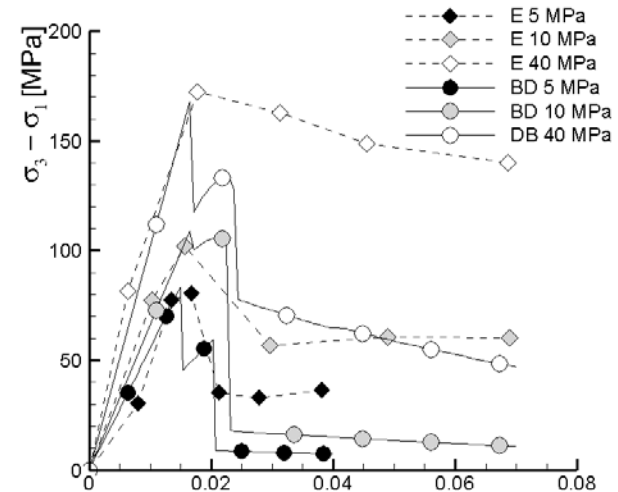
Material-point validation: Beishan granite

- Experimental data from [Ma et al., 2012]
- Confinement 10 MPa
- Triaxial test up to the peak, with measurements of the permeability
- Missing material data on resistance and fracture energy
- Satisfactory deviatoric stress versus axial and lateral strain
- Prediction of permeability shows sharp upturn followed by recovery after peak, corresponding to usual experimental trend



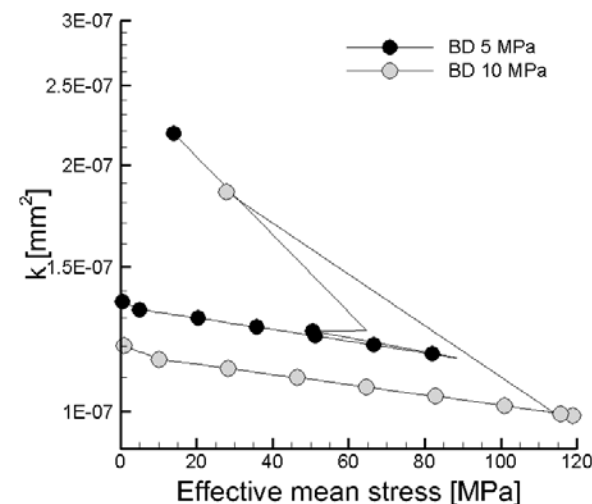
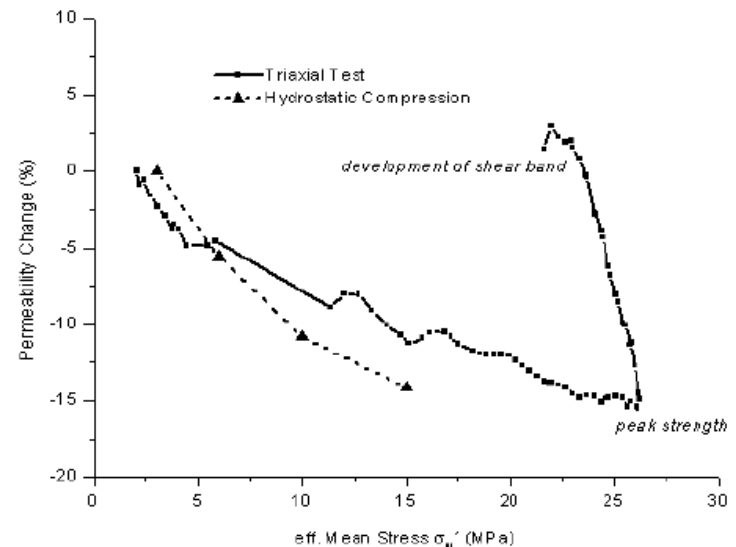
Material-point validation: Berea sandstone

- Experiments from [Zhu & Wong, 1997]
- Triaxial tests with post-peak measurements of porosity and permeability
- Missing the data on strength and fracture energy
- Confinement 5, 10 and 40 MPa
- Good agreement on the stress-strain curves for all levels of confinement
- Good agreement on the porosity curves, especially for the lower confinement, showing decrease during loading and recovery during unloading



Material-point validation: Berea sandstone

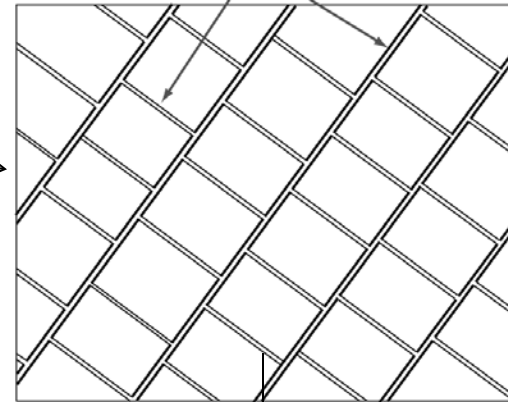
- Experiments from [Zhu & Wong, 1997]
- Triaxial tests with post-peak measurements of porosity and permeability
- Missing the data on strength and fracture energy
- Confinement 5, 10 and 40 MPa
- Good agreement on the stress-strain curves for all levels of confinement
- Predicted permeability shows decrease during loading and recovery during unloading, in agreement with usual experimental trend



Concluding remarks

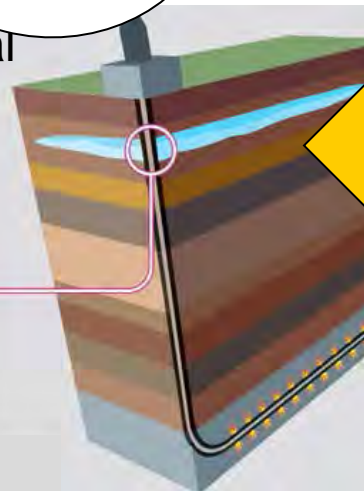
Hydraulic Fracture (HF) is characterized by complex, multiscale, multiphysics behavior

subgrid model

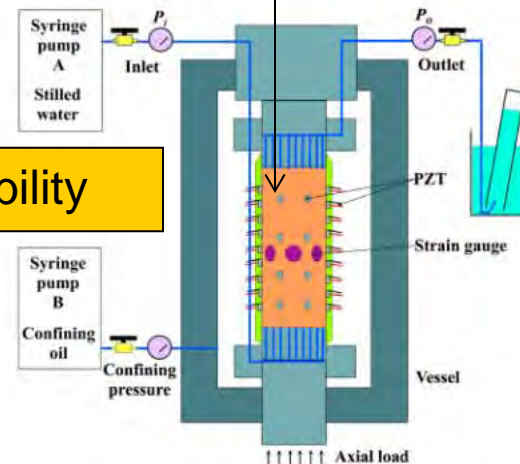


environmental impact analysis

Freshwater aquifers, which typically lie no deeper than 100 metres underground, are protected from possible pollution from the wellbore by triple-layered steel casings



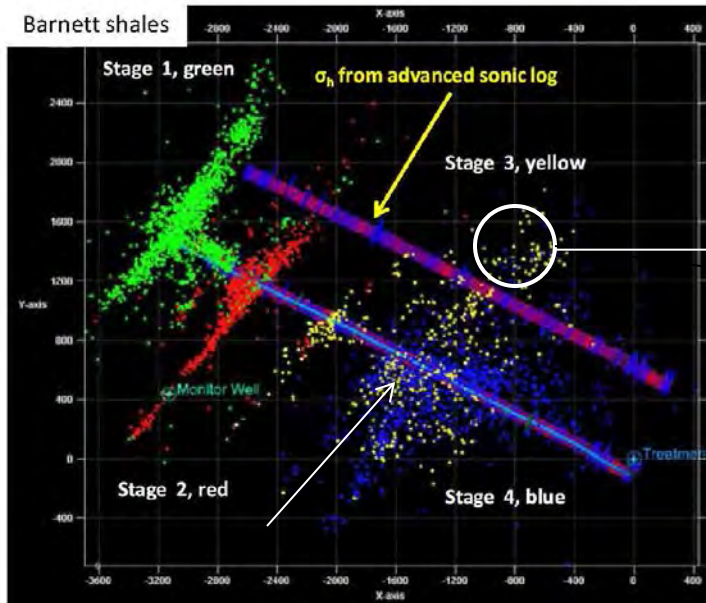
permeability



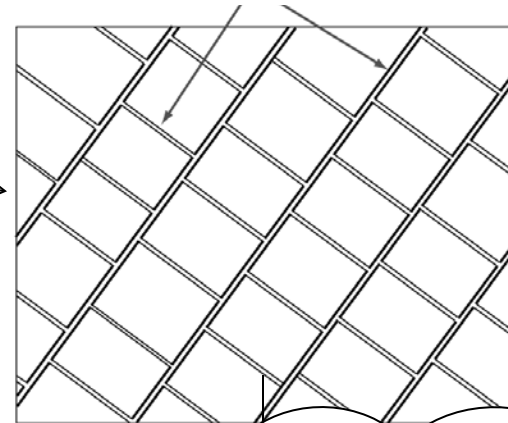
Lei et al., *Geophys. Res. Lett.*,
38, L24310, 2011

Paris, June 3, 2015

Concluding remarks

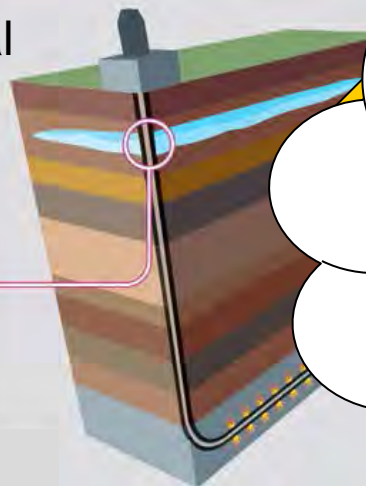


subgrid model



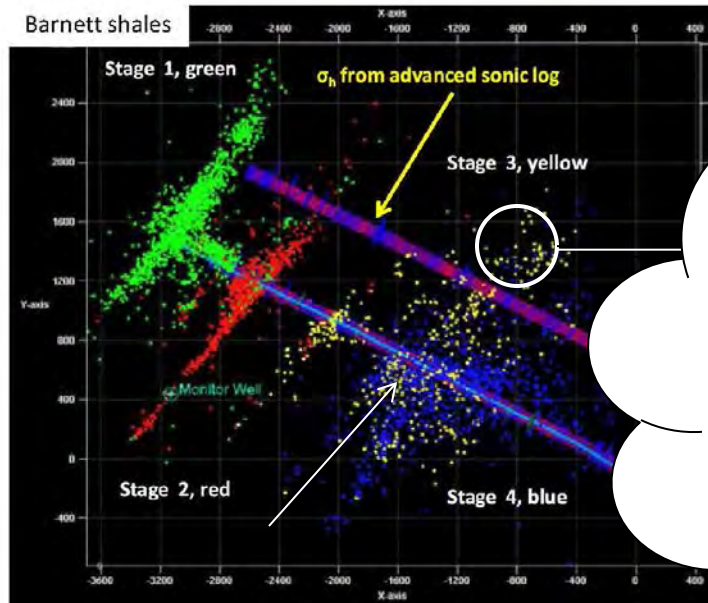
environmental
impact
analysis

Freshwater aquifers, which typically lie no deeper than 100 metres underground, are protected from possible pollution from the wellbore by triple-layered steel casings



*Permeability depends
on fine structure of
fracture patterns
(no only averages)*

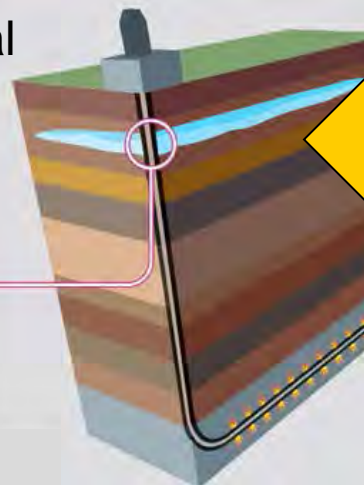
Concluding remarks



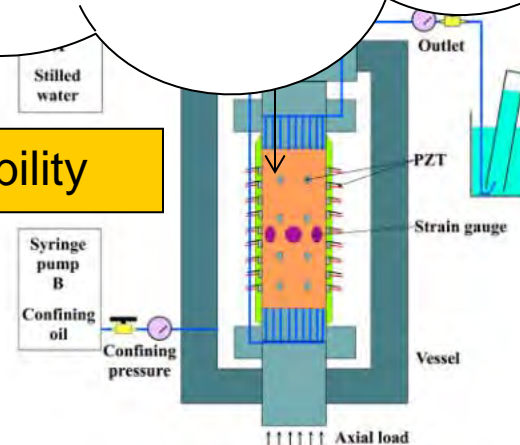
Sequential faulting is optimal at relaxing geostatic stresses

environmental impact analysis

Freshwater aquifers, which typically lie no deeper than 100 metres underground, are protected from possible pollution from the wellbore by triple-layered steel casings



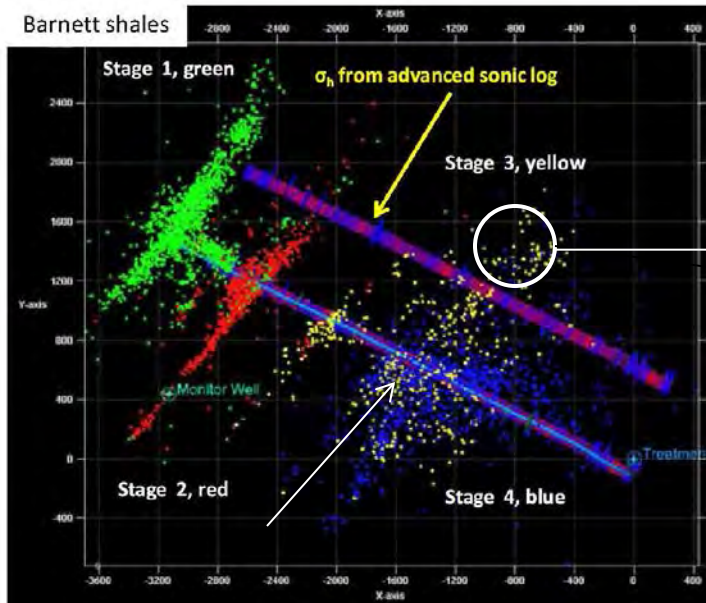
permeability



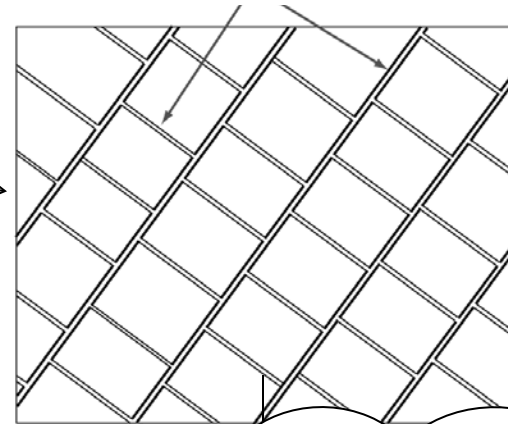
Lei et al., *Geophys. Res. Lett.*,
38, L24310, 2011

Paris, June 3, 2015

Concluding remarks

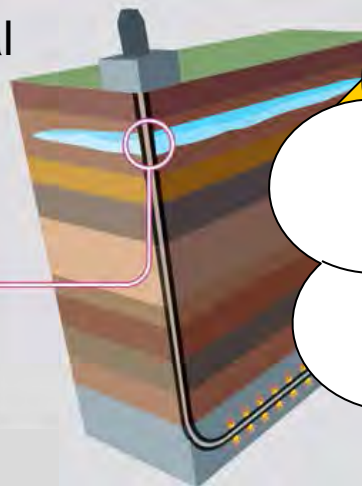


subgrid model



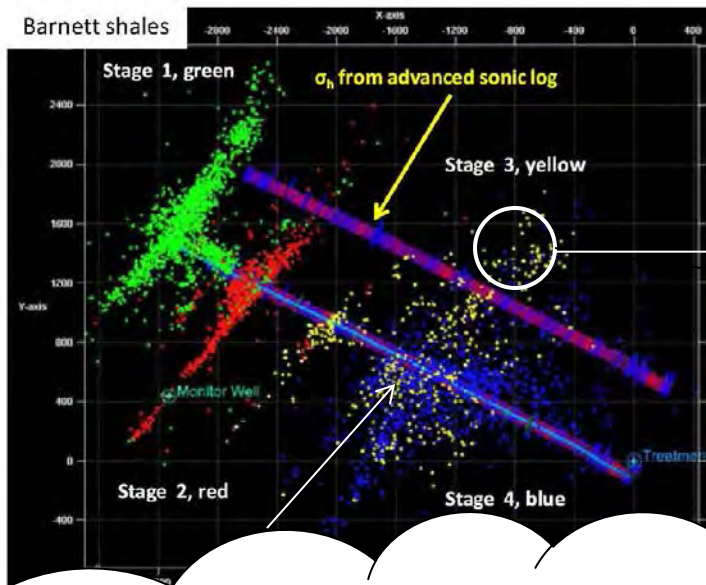
environmental
impact
analysis

Freshwater aquifers, which typically lie no deeper than 100 metres underground, are protected from possible pollution from the wellbore by triple-layered steel casings

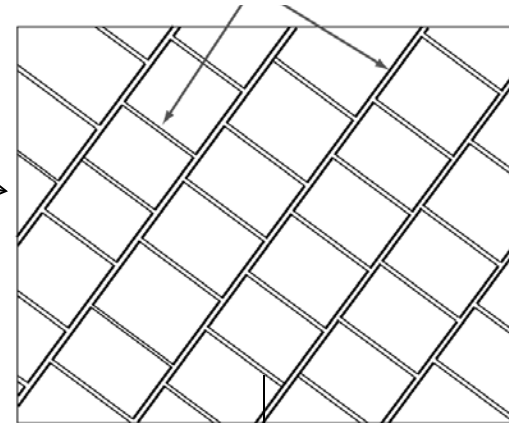


*Sequential faulting
introduces channels for
fluid flow, resulting in
enhanced permeability*

Concluding remarks

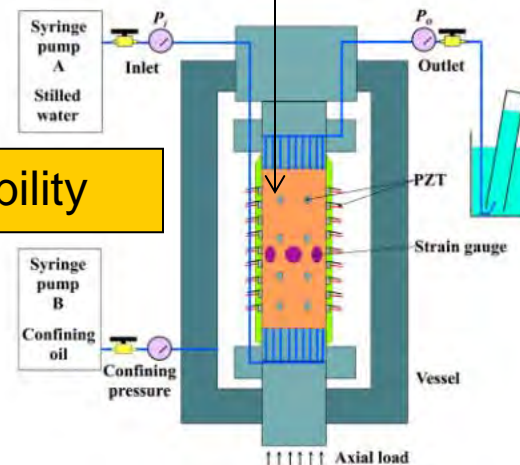


subgrid model



Potential payoff: HF process optimization, environmental impact (microseismicity, waste fluid disposal...)

ability



Lei et al., *Geophys. Res. Let.*,
38, L24310, 2011

Paris, June 3, 2015

Concluding remarks

Thank you!